research papers

Structures of (S)-(−)-4-oxo-2-azetidinecarboxylic acid and 3-azetidinecarboxylic acid from powder synchrotron diffraction data

Asiloé J. Mora,[a]***** Michela Brunelli,**[b] **Andrew N. Fitch,**[b,c] **Jonathan Wright,**[b] **Maria E. Báez**[a] **and Francisco López-Carrasquero**[a]

[a]Departamento de Química, Facultad de Ciencias, Universidad de Los Andes, Mérida 5101, Venezuela, [b]European Synchrotron Radiation Facility, BP220, F-38043 Grenoble CEDEX, France, and [c]Department of Chemistry, Keele University, Staffordshire ST5 5BG, England

Correspondence e-mail: asiloe@ula.ve

The crystal structures of the four-membered heterocycles (S)-(−)-4-oxo-2-azetidinecarboxylic acid (I) and 3-azetidinecarboxylic acid (II) were solved by direct methods using powder synchrotron X-ray diffraction data. The asymmetry of the oxoazetidine and azetidine rings is discussed, along with the hydrogen bonding.

1. Introduction

(S)-4-(−)-Oxo-2-azetidinecarboxylic acid (I) and 3-azadine-carboxylic acid (II) are strained four-membered heterocycles, difficult to synthesize owing to unfavorable enthalpies of activation (Huszthy et al., 1993). Compound (I) is an optically active β-lactam derivative of L-aspartic acid, which can be prepared by hydrogenation from (S)-4-(−)-benzyloxy-carbonyl-2-azetidinone (Fritz et al., 1986), and by oxidation of 4-vinyl-2-azetidinone (Pietsch, 1976). Derivatives of (I) are of potential interest as precursors to β-lactam antibiotics, since they can be converted into 4-acetoxy-2-azetidinones. These compounds have been recognized as the most useful precursors for the synthesis of carbapenems (Nagao, Kumagai et al., 1992; Nagao, Nagase, Kumagai, Kuramoto et al., 1992; Nagao, Nagase, Kumagai, Matsunaga et al., 1992), powerful antibiotics widely used in the pharmaceutical industry. Optically active monosubtituted alkoxycarbonyl derivatives of (I) yield helical poly β-peptides by anionic ring-opening polymerization (López-Carrasquero et al., 1994). The helical conformations adopted by these polyaspartates are similar to the α-helix of polypeptides and proteins, and they display piezoelectric and liquid crystal properties (López-Carrasquero et al., 1995; Prieto et al., 1989; Muñoz-Guerra et al., 2002). The propensity for cleavage of the amide bonds has been acknowledged, and, for instance, this feature has been used in the synthesis of a linear polyamide with hydroxymethyl pendant by the selective reduction of the 2-azetidinone moiety in the polymer main chain (Sudo et al., 2001). Compound (II) corresponds to a group of amino acids whose biological activity has been widely recognized. For example, the naturally occurring L-(2)-azeti-dinecarboxylic acid is homologous to proline (Berman et al., 1969) and mugineic acid regulates the iron intake in grami-naceous plants (Ma & Nomoto, 1996; Mino et al., 1983). On the other hand, many efforts have been directed towards the development of conformationally constrained analogs of essential animoacids (Hanessian et al., 1999) and peptido-mimetics (Alonso et al., 2001) that display more favorable pharmaceutical properties. Here we report the structures of two compounds with prospective applications in those fields. The crystal structures were solved from powder diffraction data and will be discussed in the light of 6–31+G(d) *GAUS-*

Table 1
Experimental details.

	(I)	(II)
Crystal data		
Chemical formula	$C_4H_5O_3N$	$C_4H_7O_2N$
M_r	114.68	101.11
Cell setting, space group	Orthorhombic, $P2_12_12_1$	Monoclinic, $P2_1$
Temperature (K)	295	295
a, b, c (Å)	8.94684 (2), 7.6696 (2), 7.2755 (2)	6.27983 (3), 7.8380 (1), 5.46296 (3)
β (°)	90	114.893 (1)
V (Å)	499.24 (1)	243.91 (1)
Z	4	2
D_x (Mg m^{-3})	1.531 (1)	1.377 (1)
Radiation type	Synchrotron	Synchrotron
Incident radiation wavelength (Å)	0.84933	0.540211
μ (mm^{-1})	0.16	0.07
Specimen form, color	Cylinder (particle morphology: thin powder), white powder	Cylinder (particle morphology: thin powder), white powder
Specimen size (mm)	1.5 × 40	1.5 × 40
Specimen preparation temperature (K)	Room temperature	Room temperature
Data collection		
Diffractometer	Beam line ID31, ESRF	Beam line ID31, ESRF
Data collection method	Specimen mounting: borosilicate glass capillary; mode: transmission; scan method: continuous	Specimen mounting: borosilicate glass capillary; mode: transmission; scan method: continuous
Absorption correction	None	None
2θ (°)	$2\theta_{min} = 7.0$, $2\theta_{max} = 43.5$, increment = 0.003	$2\theta_{min} = 5.0$, $2\theta_{max} = 32.0$, increment = 0.003
Refinement		
R-factors R_p, R_{wp}, R_{exp}	0.0594, 0.0861, 0.0308	0.0592, 0.0732, 0.0376
Wavelength of incident radiation (Å)	0.84933	0.54021
Excluded region(s)	None	None
Profile function	CW profile function number 3 with 19 terms	CW profile function number 3 with 19 terms
No. of parameters	76	85
$(\Delta/\sigma)_{max}$	0.92	1.66

Computer programs used: *EXPO-SIRPOW* (Altomare *et al.*, 1999), *GSAS* (Larson & Von Dreele, 2001).

*SIAN*94 (Frisch *et al.*, 1995) geometrical optimizations and the formation of hydrogen bonds.

(I)   (II)
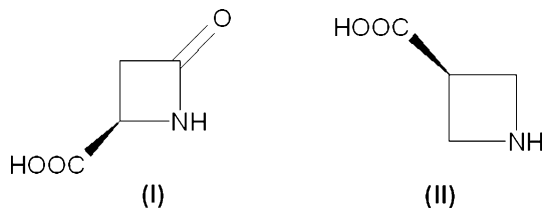
2. Experimental

2.1. Synthesis of (S)-(−)-4-oxo-2-azetidinecarboxylic acid (I)

(S)-4-Benzyloxycarbonyl-2-azetidinone was prepared as the starting material from L-aspartic acid (Aldrich, 98+%, $[a]_D^{25} = +25$) according to literature methods (Rodríguez-Galán *et al.*, 1986). In a PARR hydrogenator, 1 g (4.9 mmol) of (S)-4-(−)-benzyloxycarbonyl-2-azetidinone dissolved in 20 ml of *i*-propanol was hydrogenated over Pd/C to 5% (86 mg) at room temperature and 1.5 atm for 15 to 20 min. After this time, the catalyst was filtered from the solution and most of the solvent evaporated. Hexane was added to the residual mixture, which was allowed to crystallize at room temperature. The (S)-(−)-4-oxo-2-azetidinecarboxylic acid yield was 0.48 g (85%), m.p. 375–377 K Lit. (Frits) 375–377 K. IR (KBr): 3339, 1747, 1729, 1211, 1196, 1166 cm^{-1}. ^{1}H NMR (in DMSO-d_6) δ(p.p.m.): 7.5 (br, 1H N**H**); 4.2 (dd, 1H, C**H**NH), 3.3 (ddd, 1H, C**H**$_2$CO), 3.0 (ddd, 1H, C**H**$_2$CO). $[\alpha]_D^{20} = -80°$; $c = 1$ in water (Fritz *et al.*, 1986).

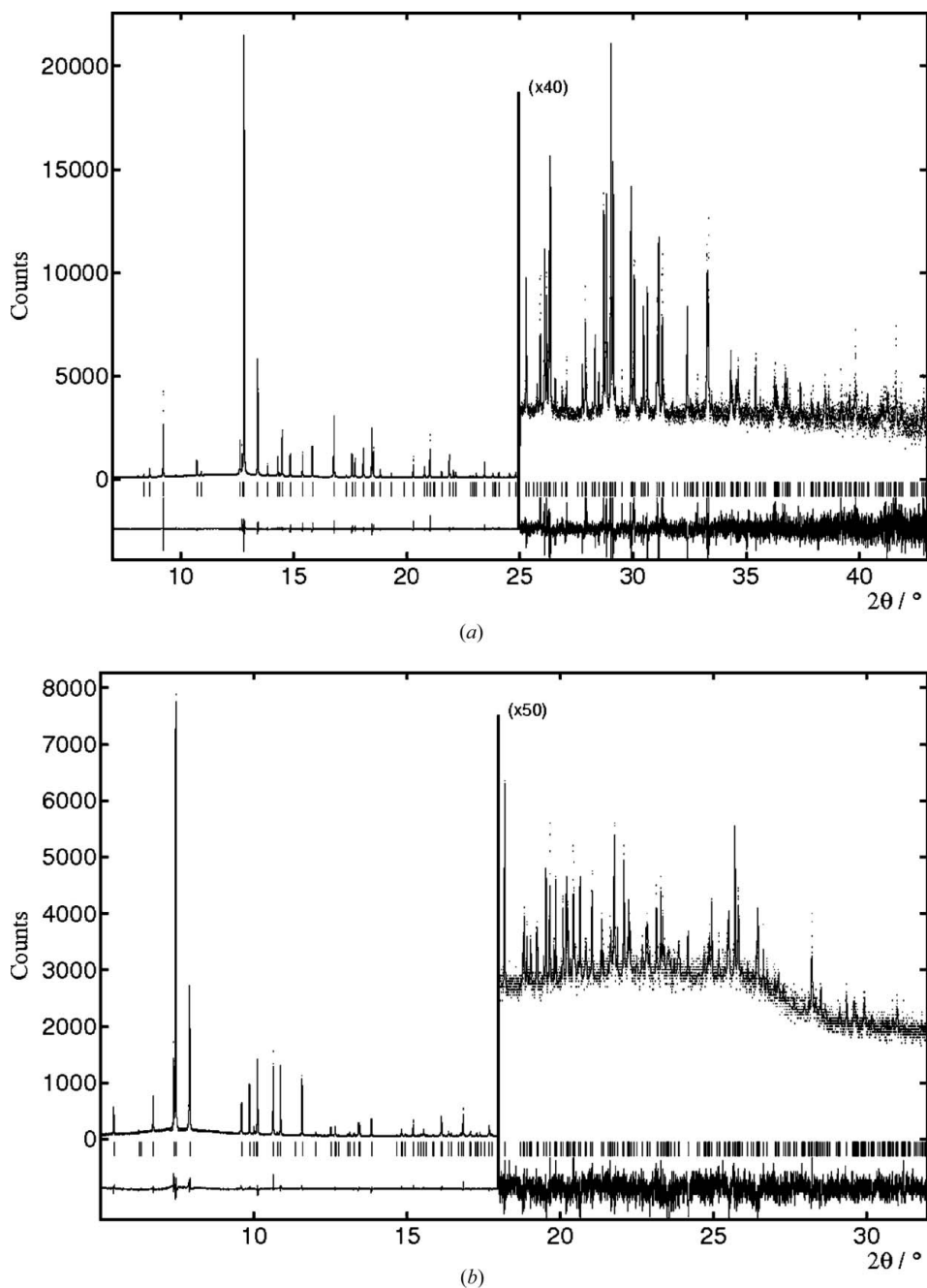### 2.2. Powder data collection

X-ray powder diffraction data were collected with the high-resolution X-ray powder diffractometer on beamline BM16 at ESRF (Fitch, 2004), selecting X-rays from the white bending magnet source with wavelengths of 0.84933 (1) and 0.54021 (1) Å for (I) and (II), respectively. Small quantities of (I) and (II) (Aldrich, 98%) were lightly ground with a pestle in an agate mortar and introduced into 1.5 mm diameter borosilicate glass capillaries, mounted on the axis of the diffractometer and spun during measurements. Data were collected for several hours and normalized against monitor counts and detector efficiencies, and rebinned into steps of $2\theta = 0.003°$.

3. Results

3.1. Structural solution and refinement

The diffraction pattern of the β-lactam (I) was indexed in an orthorhombic cell with $a = 8.9468$ (2), $b = 7.66956$ (2) and $c = 7.27555$ (2) Å (refined values) [DICVOL91 (Boultif & Louër, 1991), with indexing figures of merit: $M(20) = 60.0$ (de Wolff, 1968) and $F(20) = 281.1$ (Smith & Snyder, 1979)]. Evaluation of the systematic absences in the diffraction pattern indicated the space group $P2_12_12_1$ (No. 19), with $Z = 4$. The pattern decomposition using the Le Bail method (LeBail *et al.*, 1988) and the crystal structure solution *via* direct methods were obtained using the program *EXPO* (Altomare *et al.*, 1999). The azetidinecarboxylic acid (II) was also obtained as a pure phase and its powder diffraction pattern was indexed by a monoclinic cell: $a = 6.27985$ (3), $b = 7.8310$ (1), $c =$

(a)

(b)

Figure 1
Final observed (points), calculated (lines) and difference profiles of the Rietveld plot for (a) (S)-(−)-4-oxo-2-azetidinecarboxylic acid (I) and (b) 3-azetidinnecarboxylic acid (II).

$P2_1$ cell gave as the best solution the positions of all the non-H atoms. Both models were completed placing the H atoms with the sketching facilities of *MATERIALS STUDIO* (Accelrys Inc., 2001). Rietveld (1969) refinement of the structures were performed with the program *GSAS* (Larson & Von Dreele, 2001).

For lactam (I), data in the 2θ range 7–43° were included, comprising 218 Bragg reflections, which were modeled using a pseudo-Voigt peak-shape function (Thompson *et al.*, 1987). This function included the axial divergence asymmetry correction at low angle (Finger *et al.*, 1994). The background was described by the automatic interpolation of 20 points throughout the whole pattern. In order to place the appropriate bond and angle restraints on the model, a search of the Cambridge Crystallographic Database (CSD; Allen, 2002) was performed and five 2-acetidinone fragments were found (FEPNAP, EABLEY, FEHWOE, REPLON and VUJHOX). No regular pattern of asymmetry in the four-membered rings could be recognized since distances and bond angles varied depending on the substitute groups. Therefore, it was considered more accurate to restrain the model using the bond lengths and angles obtained in an *ab initio* molecular-orbital optimization of (I), using *GAUSSIAN*94 (Frisch *et al.*, 1995 with a 6–31 +G(d) basis set. Bond and angle restraints were weighted by 0.05 Å and 5.00°, respectively. H atoms were refined with C−H, N−H and O−H distances restrained to be 0.99 Å (weighted 0.05 Å). The isotropic displacement parameters for all H atoms were refined individually. The refinement of 73 parameters yielded final agreement factors: $R_{wp} = 0.0861$ and $R_{exp} = 0.0308$.

For the structure of compound (II), 295 reflections were refined following the procedure described above. Detailed crystallographic information and final Rietveld refinement

5.46296 (3) Å and $\beta = 114.893 (1)°$ (refined values) [DICVOL91 (Boultif & Louër, 1991), with indexing figures of merit: $M(20) = 75.8$ (de Wolff, 1968) and $F(20) = 390.4$ (Smith & Snyder, 1979)]. Analysis of systematic absences gave two possible space groups: $P2_1$ (No. 4) and $P2_1/m$ (No. 11). Statistical analysis of the reflection intensities distribution performed by the *EXPO* suite of programs (Altomare *et al.*, 1999) ruled out the centrosymmetric space group, and running the direct methods routine of *EXPO* in default mode in the

Table 2
Selected bond distances (Å) and angles (°).

	(I)	6-31G(d) MO calculations	(II)	6-31G(d) MO calculations
O1—C3	1.190 (4)	1.180		
O2—C4	1.319 (4)	1.320	1.238 (5)	1.240
O3—C4	1.208 (4)	1.180		
O1—C4			1.263 (6)	1.240
N1—C1	1.483 (4)	1.464		
N1—C3	1.378 (4)	1.386	1.462 (6)	1.460
N1—C2			1.460 (5)	1.460
C1—C2	1.585 (4)	1.550	1.551 (7)	1.550
C2—C3	1.554 (5)	1.530		
C1—C3			1.542 (14)	1.550
C1—C4	1.548 (4)	1.520	1.556 (6)	1.520
C1—C2—C3	84.3 (2)	85		
C3—N1—C1	94.7 (2)	95		
C2—N1—C3			90.4 (1)	90
C2—C1—C3			84.0 (1)	85
N1—C1—C2	87.9 (2)	88		
N1—C3—C2	93.0 (2)	92		
N1—C2—C1			92.6 (1)	92
N1—C3—C1			92.9 (1)	92
O3—C4—C1—N1	−5.6 (4)			
O3—C4—C1—C2	−107.6 (3)			
O2—C4—C1—N1	177.3 (2)			
O2—C4—C1—C2	75.3 (3)		133.6 (6)	
O2—C4—C1—C3			84.1 (6)	
O1—C4—C1—C3			−52.2 (8)	
O1—C4—C1—C2			−146.1 (5)	

agreement factors for both structures are summarized in Table 1. Fig. 1 shows the final Rietveld plots for the β-lactam (I) and the azetidinecarboxylic acid (II), respectively.

4. Discussion

Fig. 2 shows the molecular conformation and atom-labeling scheme for both compounds. Table 2 depicts the selected bond distances, angles and torsion angles for (I) and (II) compared with those obtained by theoretical *ab initio* calculations. The carboxylic O2—C3 and O3—C3 bond distances in the β-lactam (I) are markedly different, while those distances are equal within 5σ in the 3-azedinecarboxylic acid (II). These results are clear evidence that at room temperature compound (I) is a neutral species, while compound (II) is a zwitterion. The β-lactam ring in (I) is highly asymmetrical owing to the chiral environment around N1 (see bond distances N1—C1, N1—C3, C2—C3 and C1—C2, and related angles) and flat with maximum deviations of ±0.013 Å from the mean plane. This planarity is promoted by the sp^2 states of C3 and N1. O1 lies close to the β-lactam plane at 0.039 Å, while C4 is out of the plane by 1.176 Å. In contrast, the azetidine ring in (II) is almost symmetrical (see bond distances N1—C3, N1—C2, C1—C2 and C1—C3, and related angles), with a pseudo-mirror plane passing through N1 and C1 atoms, due mainly to the acidic substitution in C1, opposite to N1. The azetidine

ring is also planar with maximum deviations of −0.018 and +0.017 Å from the mean plane. In this case, C4 is out of the plane by 1.272 Å. The orientation of the carboxylic acid with respect to the ring in both structures can be explored by means of torsion angles about the C1—C4 bond. In the β-lactam (I), torsion angles N1—C1—C4—O3 −5.63 and N1—C1—C4—O2 177.25° indicate that the bonds C4—O3 and C4—O2 are aligned with the C1—N1 bond of the ring. In the 3-azetidine-carboxylic acid (II), O1 and O2 are positioned almost symmetrically with respect to the ring, being part of the pseudo-mirror plane passing through N1—C1, as depicted by the torsion angles C3—C1—C4—O1 146, C2—C1—C4—O2
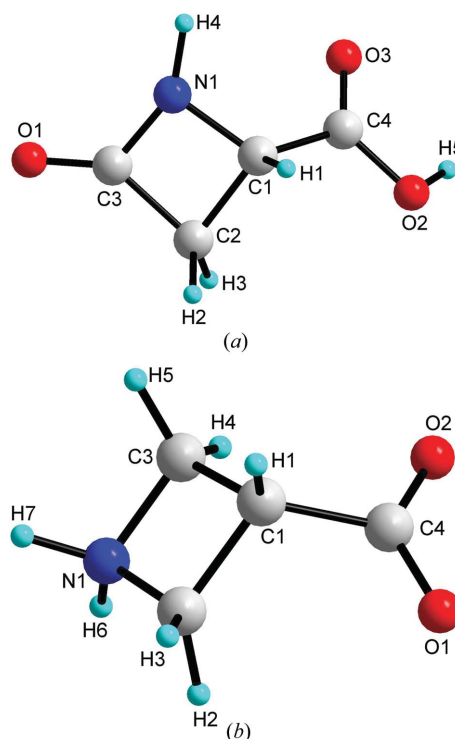

(a)

(b)

Figure 2
Molecular diagrams for (a) (S)-(−)-4-oxo-2-azetidinonecarboxylic acid (I) and (b) 3-azetidinnecarboxylic acid (II), showing the atom-labeling scheme.
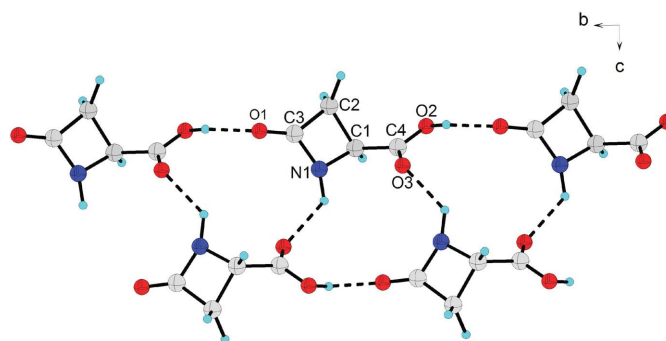

Figure 3
Extended ribbon supramolecular structure constructed from hydrogen bonds in (S)-(−)-4-oxo-2-azetidinecarboxylic acid (I).

Table 3
Geometries of hydrogen bonds (Å, °).

$D—H\cdots A$	$D—H$	$H\cdots A$	$D\cdots A$	$D—H\cdots A$
(S)-4-(−)-Oxo-2-azetidinecarboxylic acid (I)				
N1—H4$\cdots$O3[i]	1.05 (2)	2.13 (2)	2.933 (4)	132 (1)
O2—H5$\cdots$O1[ii]	0.97 (4)	1.75 (4)	2.573 (3)	141 (3)
C2—H2$\cdots$O3[iii]	1.10 (2)	2.55 (2)	3.320 (4)	127 (1)
C2—H3$\cdots$O1[iv]	1.17 (2)	2.34 (2)	3.351 (4)	143 (1)
3-Azetidinnecarboxylic acid (II)				
N1—H6$\cdots$O1[v]	1.0 (2)	1.59 (2)	2.671 (4)	178 (3)
N1—H7$\cdots$O1[vi]	1.03 (3)	2.58 (3)	3.262 (4)	123 (2)
N1—H7$\cdots$O2[vi]	1.03 (3)	1.69 (3)	2.718 (5)	175 (1)
C1—H1$\cdots$O2[vii]	1.05 (2)	2.28 (2)	3.259 (2)	155 (3)
C2—H2$\cdots$O2[viii]	1.03 (3)	2.46 (3)	3.475 (6)	168.5 (9)
C3—H5$\cdots$O1[ix]	1.08 (3)	2.39 (2)	3.440 (6)	166 (1)

Symmetry codes: (i) $1-x, -\frac{1}{2}+y, -\frac{1}{2}+z$; (ii) $x, 1+y, z$; (iii) $\frac{1}{2}+x, \frac{1}{2}-y, -z$; (iv) $1-x, \frac{1}{2}+y, \frac{1}{2}-z$; (v) $1-x, \frac{1}{2}+y, 1-z$; (vi) $-1+x, y, -1+z$; (vii) $1-x, -\frac{1}{2}+y, 2-z$; (viii) $x, y, -1+z$; (ix) $-1+x, y, z$.
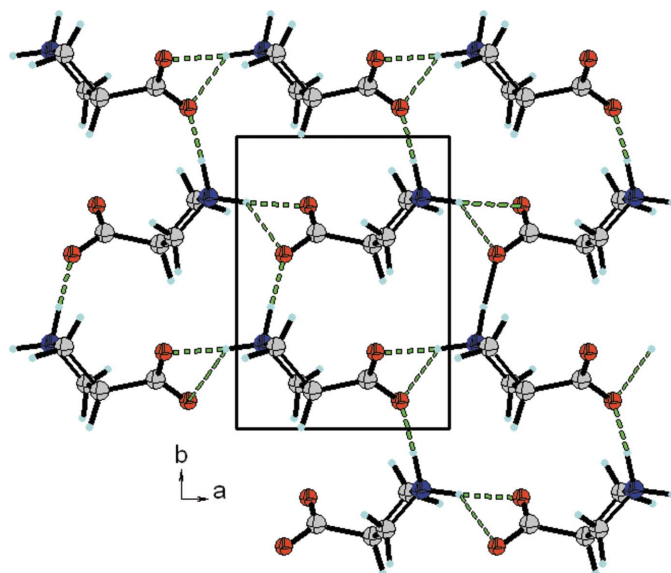

Figure 4
Projection down [001] for 3-azetidinnecarboxylic acid (II) showing the hydrogen-bonding scheme.

−134, C3—C1—C4—O2 −39.8 and C2—C1—C4—O1 −52.4°.

The slightly slacker constraints applied to the geometry of the 4-atom rings allowed them to reach the geometry that best fitted the diffraction data. In this regard, both compounds displayed the same asymmetry pattern shown by the theoretically calculated molecules. However, a closer analysis of the theoretical and X-ray diffraction distances of Table 2 show that for the β-lactam (I) there is an elongation of *ca* 0.03 Å of the C1—N1 and C1—C2 distances nearer to the pendant carboxylic acid group at C1, which also shows a C1—C4 distance longer than that calculated by 0.036 Å. This could be associated with the librational thermal motion of the molecule. In the case of (II) this elongation is only observed in the C1—C4 bond of the carboxylate group pending group. This thermal motion cannot be modeled from powder diffraction data due

to the well known limitations arising from the overlap of reflections, particularly at higher diffraction angles.

Hydrogen bonds for both compounds are summarized in Table 3. In the β-lactam (I), a supramolecular bidimensional structure is recognized, as shown in Fig. 3. Extended chains constructed with strong O2—H5$\cdots$O1 hydrogen bonds run parallel to [010]. Additional N1—H4$\cdots$O3 hydrogen bonds link neighboring chains laterally forming ribbons also running parallel to [010]. As observed in previous studies (Mora *et al.*, 2005), the four hydrogen-bond acceptor capacity of the carboxylic acid is completed by means of two weak C2—H2$\cdots$O3 and C2—H3$\cdots$O1 hydrogen bonds. Hydrogen bonding in the 3-azetidinecarboxylic acid (II) is markedly different because of its zwitterionic characters, which makes the amine group in the ring a double donor of H atoms. In fact, a two-dimensional network of hydrogen bonds is assembled by the combination of two motifs: infinite two-membered zigzag chains connected by N1—H6$\cdots$O1 hydrogen bonds running along **b**, and infinite one-membered chains running along [101] connected by a bifurcated hydrogen bond N1—H7$\cdots$O1 and N1—H7$\cdots$O2. A perspective view of this hydrogen-bond network is shown in Fig. 4. In addition, some weak C—H$\cdots$O hydrogen bonds are also present, which saturates the acceptor capacity of the carboxylate group.

References

Accelrys Inc. (2001). *MATERIALS STUDIO*. Accelrys Inc., 6985 Scranton Road, San Diego, CA 92121–3752, USA.
Allen, F. H. (2002). *Acta Cryst.* B**58**, 380–388.
Alonso, E., López-Ortiz, F., del Pozo, C., Peralta, E., Macías, A. & González, J. (2001). *J. Org. Chem.* **66**, 6333–6338.
Altomare, A., Burla, M. C., Camalli, M., Carrozzini, B., Cascarano, G. L., Giacovazzo, C., Guagliardi, A., Moliterni, A. G. G., Polidori, G. & Rizzi, R. (1999). *J. Appl. Cryst.* **32**, 339–340.
Berman, H. M., McGandy, E. L., Burgner, J. W. & VanEtten, R. L. (1969). *J. Am. Chem. Soc.* **91**, 6177–6182.
Boultif, A. & Louër, D. (1991). *J. Appl. Cryst.* **24**, 987–993.
Finger, L. W., Cox, L. W. & Jephcoat, A. P. (1994). *J. Appl. Cryst.* **27**, 892–900.
Fitch, A. N. (2004). *Res. Natl. Inst. Stand. Technol.* **109**, 133–142.
Frisch, M. J. *et al.* (1995). *GAUSSIAN*. Gaussian Inc., Pittsburgh, PA, USA.
Fritz, H., Sutter, P. &. Weis, C. D. (1986). *J. Org. Chem.* **51**, 558–561.
Hanessian, S., Bernstein, N., Yang, R.-Y. & Maguire, R. (1999). *Bioorg. Med. Chem. Lett.* **9**, 1437–1442.
Huszthy, P., Bradshaw, J. S., Krakowiak, K. E.,Wang, T. & Dalley, N. K. (1993). *J. Heterocycl. Chem.* **30**, 1197–1207.
Larson, A. C. & Von Dreele, R. B. (2001). *GSAS*. Los Alamos National Laboratory, Los Alamos, New Mexico, USA.
LeBail, A., Duroy, H. & Fourquet, J. L. (1988). *Mater. Res. Bull.* **23**, 447–452.
López-Carrasquero, F., Aleman, C. & Muñoz-Guerra, S. (1995). *Biopolymers*, **36**, 263–271.
López-Carrasquero, F., García-Álvarez, M. & Muñoz-Guerra, S. (1994). *Polymer*, **35**, 4502–4510.
Ma, J. F. & Nomoto, K. (1996). *Physiol. Plant*, **97**, 609–617.

Mora, A. J., Avila, E. E., Delgado, G. E., Fitch, A. N. & Brunelli, M. (2005). *Acta Cryst.* B**61**, 96–102.

Muñoz-Guerra, S., López-Carrasquero, F., Alemán, C., Morillo, M., Castelleto, V. & Hamley, I. (2002). *Adv. Mater.* **14**, 203–205.

Mino, Y., Ishida, T., Ota, N., Inoue, N., Nomoto, K., Takemoto, T., Tanaka, H. & Sugiura, Y. (1983). *J. Am. Chem. Soc.* **105**, 4671–4676.

Nagao, Y., Kumagai, T., Nagase, Y., Tamai, S., Inoue, Y. & Shiro, M. (1992). *J. Org. Chem.* **57**, 4232–4237.

Nagao, Y., Nagase, Y., Kumagai, T., Kuramoto, Y., Kobayashi, S., Inoue, Y., Taga, T. & Ikeda, H. (1992). *J. Org. Chem.* **57**, 4238–4242.

Nagao, Y., Nagase, Y., Kumagai, T., Matsunaga, H., Abe, T., Shimada, O., Hayashi, T. & Inoue, Y. (1992). *J. Org. Chem.* **57**, 4243–4249.

Pietsch, H. (1976). *Tetrahedron Lett.* pp. 4053–4056.

Prieto, A., Pérez, R. & Subirana, J. A. (1989). *J. Appl. Phys.* **66**, 803–806.

Rietveld, H. M. (1969). *J. Appl. Cryst.* **2**, 65–71.

Rodríguez-Galán, A., Muñoz-Guerra, S., Subirana, J. A., Chuong, B. & Sekiguchi, H. (1986). *Makromol. Chem. Macromol. Symp.* **6**, 277–284.

Smith, G. S. & Snyder, R. L. (1979). *J. Appl. Cryst.* **12**, 60–65.

Sudo, A., Sato, M. & Endo, T. (2001). *J. Polym. Sci.* **39**, 3789–3796.

Thompson, P., Cox, D. E. & Hastings, J. B. (1987). *J. Appl. Cryst.* **20**, 79–83.

Wolff, P. M. de (1968). *J. Appl. Cryst.* **1**, 108–113.